2-5 pyrochlore relaxor ferroelectric Cd2Nb2O7 and its Fe2+/Fe3+ modifications

N. N. Kolpakova, P. P. Syrnikov, A. O. Lebedev, P. Czarnecki, W. Nawrocik, C. Perrot, L. Szczepanska

2–5 pyrochlore relaxor ferroelectric $Cd_2Nb_2O_7$ and its Fe^{2+}/Fe^{3+} modifications

N. N. Kolpakova,[a] P. P. Syrnikov, and A. O. Lebedev
A. F. Ioffe Physico-Technical Institute RAS, Polytekhnicheskaya 26, 194021 St. Petersburg, Russia

P. Czarnecki, W. Nawrocik, and C. Perrot
Institute of Physics, A. Mickiewicz University, Umultowska 85, 61-614 Poznan, Poland

L. Szczepanska
Institute of Molecular Physics PAS, Smoluchowskiego 17, 60-179 Poznan, Poland

(Received 16 April 2001; accepted for publication 7 September 2001)

The weak-field dielectric dispersion (100 Hz–1.8 GHz) studies both of pure and Fe^{2+}/Fe^{3} modified $Cd_2Nb_2O_7$ ceramics over the temperature range of 90–380 K are presented and discussed from the viewpoint of relaxor and glassy properties of the system. It is revealed that $Cd_2Nb_2O_7$ pyrochlore is intolerant of the addition of 25 mol % Fe^{2+} or Fe^{3+} for Cd^{2+}. From the x-ray diffraction analysis, pure $Cd_2Nb_2O_7$ forms a single-phase pyrochlore, while the compositions $Cd_{1.5}Fe^{2+}_{0.5}Nb_2O_7$ and $Cd_{1.5}Fe^{3+}_{0.5}Nb_2O_7$ give $CdNb_2O_6$ columbite doped with Fe^{2+} or Fe^{3+} on the Cd sites (<8 and <2 mol %, respectively), except for minor amount of parasitic hematite. The novel $CdNb_2O_6$ type compounds are not ferroelectrics, unlike $Cd_2Nb_2O_7$. In the latter, at $T_C=196$ K the dielectric relaxation due to the motion of ferroelectric domain walls driven by an external ac electric field is observed. A polydispersive dielectric response of $Cd_2Nb_2O_7$ around 188 K has characteristics of the relaxor ferroelectrics with glassy behavior (like PMN). Near the characteristic freezing temperature of the zero-field-cooled state ($T_f=183$ K) the dielectric absorption spectra and the relaxation-time distribution strongly broaden and tend to flatten out, while below T_f the imaginary part of the dielectric permittivity becomes nearly frequency independent. The dielectric response of $Cd_2Nb_2O_7$ dominating far below T_C (around 150 K) and that of Fe^{2+}/Fe^{3+} doped $CdNb_2O_6$ between 90 and 380 K are typical of glass-forming systems at temperature far above T_{glass}. The relaxational process is characterized by (i) a significant frequency dependence of the peak permittivity position, (ii) non-Arrhenius behavior, and (iii) increasing asymmetry of the dielectric absorption spectrum at the low-frequency side with decreasing temperature, without broadening the relaxation-time distribution and freezing the peak-absorption frequency. It is proposed that although the nature of structural disorder in $Cd_2Nb_2O_7$ pyrochlore and Fe^{2+}/Fe^{3+} doped $CdNb_2O_6$ columbite is different, in both systems the off-center displacements of the A-site ions act as a random field and are responsible for the relaxor and dipolar glass-like behavior upon cooling. The Debye-like HF dielectric relaxation (1 MHz–1.8 GHz) observed both in $Cd_2Nb_2O_7$ and its isostructural analog $Cd_2Ta_2O_7$ at RT and higher (a centrosymmetric phase) is attributed to fluctuations in polarization of the dynamically reoriented O(7th)–Cd–O(7th) dipoles due to dynamical off-center location of Cd ions. © *2001 American Institute of Physics.* [DOI: 10.1063/1.1415540]

I. INTRODUCTION

In past decades, studies of the perovskite relaxor ferroelectrics like $PbMg_{1/3}Nb_{2/3}O_3$, $PbSc_{1/2}Ta_{1/2}O_3$, $(Pb,La)(Zr,Ti)O_3$, and $Sr_{1-x}Ca_xTiO_3$ are a topic of current interest for understanding the slowing down dynamics of polar nanoregions, the correlation between glassy and relaxor behavior of the systems, the ability for transformation of a relaxor state to a ferroelectric state, and possible applications of the materials in electronics due to strong sensitivity of their physical properties to a structural disorder as well as to the external electric field strength and frequency.[1–6] Although the perovskite relaxors identified so far are *mixed* $A(X,Z)O_3$ or $(A,M)XO_3$-type systems, $Cd_2Nb_2O_7$ which belongs to the 2–5 *undiluted pyrochlores*, $A_2^{2+}B_2^{5+}O_7$, also exhibits a relaxor behavior associated with the presence of polar nanoregions.[7–9] In perovskites, a relaxor state transforms to a ferroelectric state either spontaneously or in an external dc electric field.[1,3,4] On the contrary, in $Cd_2Nb_2O_7$ pyrochlore a relaxor state and a ferroelectric state exist simultaneously below T_C and T_s ($T_C=196$ K and $T_s=205$ K are the ferroelectric and ferroelastic phase transition temperatures, respectively).[8] This feature enables the pyrochlore relaxor ferroelectric $Cd_2Nb_2O_7$ and its modifications as the promising materials for various applications to be regarded as well.

Relaxor and glassy behavior of perovskites ($Pm3m-O_h^1$) and pyrochlores ($Fd3m-O_h^7$) attract special attention, as the high-symmetry paraelectric phase of the materials makes the great variety in the nature of structural phase transitions (PT) and the behavior of the systems on a

[a]Electronic mail: kolpakova@pop.ioffe.rssi.ru

temperature and time scale possible. For complex perovskites, a *compositional* disorder in location of *X* and *Z* (or/and A/M) cations is responsible for a relaxor behavior of the system. For $Cd_2Nb_2O_7$ pyrochlore, an *orientational* disorder in alignment of the O(7th)–Cd–O(7th) dipole chains along the $[111]_{cub}$ axes due to progressive freezing the Cd ions in the off-center position with decreasing temperature is responsible for a relaxor behavior of the system. Moreover, unlike perovskites, in $Cd_2Nb_2O_7$ *a sequence* of the disordered states of different nature (relaxor, incommensurable, glassy) develops in the ferroelectric phase from T_C down to 4 K, with the correlation between these states still unclear.[8–10] Their origination is ascribed to a dynamical location of the Cd^{2+} ions reoriented at a fast rate $>10^7$ Hz over the six off-center equivalent positions at room temperature (RT).[7,10] However, so far no immediate evidence for the high-frequency dipole relaxation in the system at RT (a centrosymmetric paraelectric phase) has been presented, which remains the role of the $(CdO_8)^{n-}$ network in the process ascertainable. It should be noted that in former works the dielectric relaxation studies of $Cd_2Nb_2O_7$ were restricted by the frequency range from 100 Hz to 1 MHz.[7–13] The fact that random impurities and defects on the Cd site (A-site ions) enhance the relaxor properties of this system indicates that its behavior is influenced by a structural disorder in the $(CdO_8)^{n-}$ network.[8,11,12] The structural A-site disorder can result from a chemical heterogeneity (different ionic radii, valency, polarizability, ion deficiency), from a heterogeneous positional distribution of the ions included and from off-center location of ions. Therefore, one may expect that the A-site doping with ions of a smaller ionic radius and/or a higher cationic valency than those of Cd^{2+} will also change the relaxor properties of $Cd_2Nb_2O_7$ yet no methodical study of the relaxor properties of $Cd_2Nb_2O_7$ modified by partial substitution of other ions (e.g., transition metal ions) for Cd^{2+} has been carried out.

Here, Fe^{2+} and Fe^{3+} ions were preferred for modification of $Cd_2Nb_2O_7$ due to their significantly smaller ionic radii [$r(Fe^{2+})=0.780$ Å, $r(Fe^{3+})=0.645$ Å][14] compared to that of Cd^{2+} ($r=0.99$ Å), which was expected to affect remarkably the distortion and structural disorder in the $(CdO_8)^{n-}$ network. From the structure stability viewpoint, a specificity of $Cd_2Nb_2O_7$ pyrochlore is that the ionic size of Cd^{2+} is the smallest one permitted for the A-site cation, while the ionic size of Nb^{5+} is the largest one permitted for the B-site cation. As a result, both coordination polyhedra, $(NbO_6)^{n-}$ and $(CdO_8)^{n-}$, are highly deformed but still without becoming distorted from the D_{3d}-3m symmetry required for pyrochlore formation.[15] However, the deficient compositions $Cd_{1.75}Nb_2O_{6.75}$ and $Cd_{1.5}Nb_2O_{6.5}$ give a mixture of the $CdNb_2O_6$ columbite ($Pnca$-D_{2h}^{14}) and second phase than a pyrochlore.[16,17] On the other hand, an intriguing feature of Fe ions is also the facility to form a columbite especially during formation of the pyrochlore niobates.[18] The predisposition of $Cd_2Nb_2O_7$ to form a columbite for critical amounts of the impurity ions partially substituted for Cd^{2+} seems to be interesting itself. In the latter, the polyhedra containing Cd and Nb ions become highly distorted compared to those in pyrochlore,[14,19] which may change the relaxor and ferroelectric properties of the system. At present, in the literature there are no data about the least Fe^{2+}/Fe^{3+} additions to $Cd_2Nb_2O_7$ for $Cd_{2-x}Fe_xNb_2O_7$ niobate to fall into the columbite structure. For these reasons, the relevant Fe^{2+} or Fe^{3+} containing ceramic compositions with $x(Fe)=0.5$ were prepared and studied along with a nominally pure ceramic $Cd_2Nb_2O_7$. For comparison, $Cd_2Ta_2O_7$ pyrochlore was also chosen for study as an isostructural analogue of $Cd_2Nb_2O_7$ [$r(Nb^{5+})=0.64$ Å, $r(Ta^{5+})=0.64$ Å].[14] Contrary to the latter, $Cd_2Ta_2O_7$ undergoes only one structural PT (at $T_s=204$ K), but is not a ferroelectric.[20] From the x-ray analysis, a specificity of the crystal structure of $Cd_2Nb_2O_7$ and $Cd_2Ta_2O_7$ is that Cd ions are located dynamically in the $(CdO_8)^{n-}$ polyhedra.[21] Here, to give evidence for the dynamical off-center displacements of Cd^{2+}, the high-frequency dielectric dispersion study of ceramic $Cd_2Nb_2O_7$ and $Cd_2Ta_2O_7$ at RT and higher (a centrosymmetric phase) is performed.

The aim of this work is to examine the dielectric dispersion (100 Hz–1.8 GHz) both of pure and highly A-site modified [$x(Fe)=0.5$] $Cd_2Nb_2O_7$ over the temperature range of 90–380 K in order to clarify (i) the actuality of the A-site disorder for the relaxor and glassy behavior of the systems, (ii) the multiplicity of the dielectric relaxation processes below T_C and their nature, and (iii) the ability to enhance/suppress the relaxor and ferroelectric properties of the system. To characterize the crystalline phase of the ceramics prepared, the x-ray diffraction analysis at RT along with the differential thermal analysis (DTA), thermal gravimetry (TG) and differential thermal gravimetry (DTG) in the temperature interval from 275 to 1200 K were also carried out.

II. EXPERIMENT

Standard ceramic fabrication procedures were followed for preparation of $Cd_2X_2O_7$ (X=Nb or Ta) and chemically substituted $Cd_2Nb_2O_7$ compositions.[13,16,22] Stoichiometric mixtures of the constituent metal oxides (CdO, Nb_2O_5, Ta_2O_5, Fe_2O_3, FeO) were calcined at 900 °C for about 6 h. Then the calcined powders were milled to fine powders (particle size <0.5 μm), mixed with 2 wt % PVA binder and cold pressed into pellets of 5–10 mm in diameter and 0.5–2 mm in thickness. The pellets were sintered in platinum crucible in a saturated CdO atmosphere to prevent CdO loss. The $Cd_2Nb_2O_7$ and $Cd_2Ta_2O_7$ compositions were fired at 950 °C for 10 h, the $Cd_{1.5}Fe^{2+}_{0.5}Nb_2O_7$ and $Cd_{1.5}Fe^{3+}_{0.5}Nb_2O_7$ compositions were fired at 1000 °C for 12 h. Relative densities of the sintered ceramic pellets were 94%–96% of the theoretical value.

The x-ray diffraction (XRD) powder patterns of the sintered ceramics were obtained at room temperature using an x-ray diffractometer DRON-2 with Ni-filtered Cu $K\alpha$ radiation. The DTA, DTG, and TG scans of the samples in the temperature interval from 275 to 1200 K at a heating rate of 5 or 10 K/min were made using a Paulik–Paulik-type derivatograph. For dielectric measurements, the samples were prepared from sintered pellets by polishing the faces flat and parallel. Then, the parallel faces were electroded with silver paste. The dielectric constant and dielectric losses of the samples were measured using the LF (100 Hz–13 MHz) and

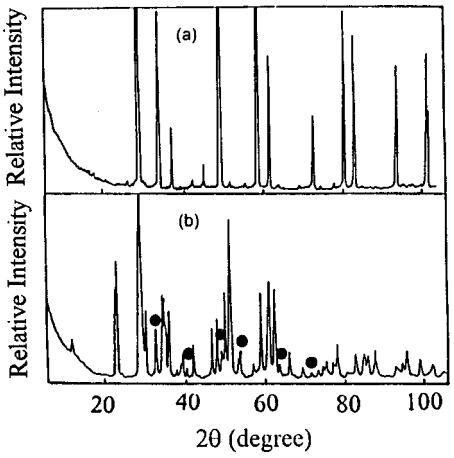

FIG. 1. XRD powder patterns of $Cd_2Nb_2O_7$ pyrochlore (a), and $Cd_{1-y}Fe_y^{3+}Nb_2O_6$ columbite (b) ceramics at RT, (●) shows the diffraction lines of hematite.

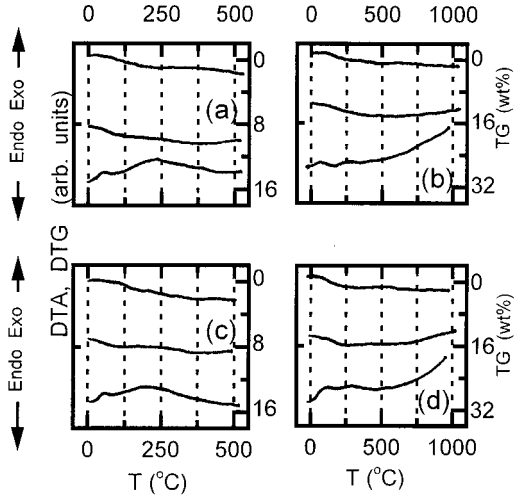

FIG. 2. DTA, thermogravimetry (TG), and differential thermogravimetry (DTG) scans of $Cd_2Nb_2O_7$ (a), $Cd_2Ta_2O_7$ (b), $Cd_{1-y}Fe_y^{3+}Nb_2O_6$ (c), and $Cd_{1-z}Fe_z^{2+}Nb_2O_6$ (d) in the temperature range from 275 to 1200 K at a heating rate of 5 K/min. For (a), (b), (c), and (d), the DTA, DTG, and TG curves are arranged from bottom to top.

rf (1 MHz–1.8 GHz) Impedance Analyzers HP-4192A and 4291A, respectively. The measurements were performed over the temperature range of 90–380 K at a slow cooling/heating rate of 0.5 or 1 K/min, with temperature controlled to within 0.1 K. The ac electric field strength was of about 4 V/cm.

III. RESULTS AND DISCUSSION

A. Characterization of the compounds

Figure 1 shows the x-ray powder diffraction (XRD) patterns of pure and Fe^{2+}/Fe^{3+} modified $Cd_2Nb_2O_7$ ceramics at RT. The XRD data for $Cd_2Nb_2O_7$ and $Cd_2Ta_2O_7$ (not shown) samples confirm a single-phase pyrochlore structure. For Fe containing compositions, the XRD patterns are identical and correspond to a mixture of two phases [Fig. 1(b)]. Because of the identity, only the XRD pattern for $Cd_{1.5}Fe_{0.5}^{3+}Nb_2O_7$ is presented in the figure. The $Cd_{1.5}Fe_{0.5}^{3+}Nb_2O_7$ and $Cd_{1.5}Fe_{0.5}^{2+}Nb_2O_7$ compositions give a mixture of the $CdNb_2O_6$ columbite ($Pnca$-D_{2h}^{14}) doped with Fe^{3+} or Fe^{2+} ions on the Cd^{2+} sites and the α-Fe_2O_3 hematite ($R\bar{3}c$-D_{3d}^6). The amount of hematite phase was $<5\%$ for Fe^{3+}-doped composition and $<3\%$ for Fe^{2+}-doped composition, respectively. Using the analytic chemistry methods, up to $\sim 2\,\text{mol}\%\,Fe^{3+}$ for $Cd_{1-y}Fe_y^{3+}Nb_2O_6$ and up to $\sim 8\,\text{mol}\%\,Fe^{2+}$ for $Cd_{1-z}Fe_z^{2+}Nb_2O_6$ were revealed.

For thermal characterization of the crystalline structure of the compounds obtained, the derivatographic measurements in the temperature interval from 275 to 1200 K were made (Fig. 2). For $Cd_2Nb_2O_7$ and $Cd_2Ta_2O_7$ [Figs. 2(a), and 2(b)], the DTA, DTG, and TG curves show an endothermic anomaly in a wide temperature interval from 250 to 800 °C. The anomaly is ascribed to the loss of H_2O and some residual reactants which still remain in the ceramics samples, with the main weight loss occurring above 400 °C (TG and DTG curves). Between 40 and 80 °C, in the DTA curves there is also a weak exothermic anomaly. The anomaly is related to the PT at $T_{tr}=46\,°C$ characteristic of $Cd_2Nb_2O_7$ and $Cd_2Ta_2O_7$ pyrochlores and caused by a change in deformation of the $(NbO_6)^{n-}/(TaO_6)^{n-}$ and $(CdO_8)^{n-}$ coordination polyhedra.[23] For Fe containing compositions [Figs. 2(c) and 2(d)], the DTA, DTG, and TG curves also show a wide endothermic anomaly in the temperature interval from 250 to 800 °C ascribed to the H_2O and some residual reactants losses, with the main weight loss occurring above 400 °C (TG and DTG curves). The exothermic anomaly in the DTA curves is observed between 40 and 80 °C for $Cd_{1-y}Fe_y^{3+}Nb_2O_6$ and between 80 and 120 °C for $Cd_{1-z}Fe_z^{2+}Nb_2O_6$. For comparison, in $FeNb_2O_6$ and $(Fe,Mn)Nb_2O_6$ columbites no apparent anomalies appear in the DTA curves up to 900 °C.[18] The anomalies observed in the Fe^{2+}/Fe^{3+} doped $CdNb_2O_6$ columbite seem to be caused by the deformation and slight change in tilting of the $(NbO_6)^{n-}$ octahedra, which occurs because the Cd^{2+} ions of a larger size then Fe^{2+} (and Fe^{3+}) ions occupy the $(AO_6)^{n-}$ octahedra. The actuality of such deformations for columbites has been reported in some earlier work.[18] The temperature at which the distortion occurs is higher for $Cd_{1-z}Fe_z^{2+}Nb_2O_6$, which can be attributed to the noteworthy deformation due to a higher amount of Fe ions included.

To elucidate the ferroelectric properties of the Fe^{2+}/Fe^{3+} doped $CdNb_2O_6$ columbite and estimate the magnitude of the spontaneous polarization $P_s(T)$, if any exists, the pyroelectric and dielectric $P-E$ hysteresis loop measurements over the temperature range of 90–290 K were performed. The data indicated no ferroelectric behavior of the compounds, except for a weak nonlinearity in the $P-E$ curves below 150 K.

So, it turned out that $Cd_2Nb_2O_7$ pyrochlore could not tolerate the addition of $25\,\text{mol}\%\,Fe^{3+}$ or Fe^{2+} for Cd^{2+}. For the novel compounds obtained, a columbite phase prevails, the XRD patterns correspond to $CdNb_2O_6$ columbite, no ferroelectric phase transition is observed down to 90 K, and the dielectric constant at RT is reduced to 30 (in $Cd_2Nb_2O_7$, $\epsilon' \sim 500$ at RT) (see Figs. 3, 9, and 10).

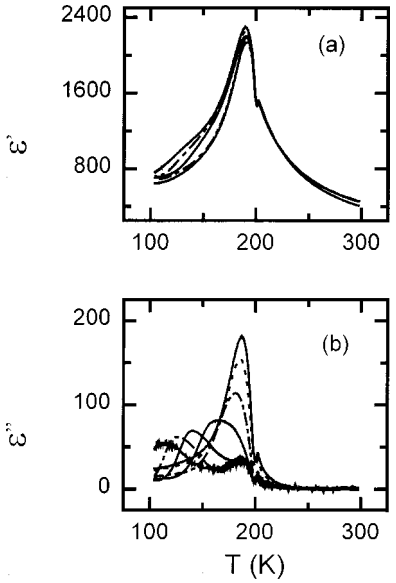

FIG. 3. Weak-field real (a) and imaginary (b) parts of permittivity as a function of temperature on cooling of pure $Cd_2Nb_2O_7$ measured at 0.8, 10, 100, 5000, and 13 000 kHz for (a) and at 0.8, 10, 100, 1000, 5000, 10 000, and 13 000 kHz for (b), from left to right.

B. Low-frequency dielectric permittivity of $Cd_2Nb_2O_7$ pyrochlore

Figure 3 shows the low-frequency (100 Hz–13 MHz) dielectric response of the pure $Cd_2Nb_2O_7$ pyrochlore as a function of frequency and temperature in the zero-field-cooled regime. The anomalies in the $\epsilon'(T)$ and $\epsilon''(T)$ curves at $T_s = 203.5$ K and $T_C = 196$ K correspond to the ferroelastic and ferroelectric PT, respectively. It should be noted that the PT at T_C is identified as the deflection point in the $\epsilon'(T)$ curves and the apparent anomaly in the $\epsilon''(T)$ curves at frequencies lower than 1 MHz, with the maximum in the $\epsilon'(T)$ curves at $T_{max} < T_C$ (see also Refs. 7–10, 13). At frequencies from 1 to 13 MHz, the peak position in the $\epsilon'(T)$ curves corresponds to T_C, while the peak position in the $\epsilon''(T)$ curves approaches steadily T_C from below. In the vicinity of T_C, the dielectric permittivity decreases and the dielectric loss increases with increasing frequency from 100 Hz to 13 MHz, which is characteristic of the dielectric response of a normal ferroelectric caused by the domain wall motions in a weak ac electric field.

Below T_C, two additional dielectric relaxation processes develop in $Cd_2Nb_2O_7$ (around 188 and 150 K) (Fig. 3). The peak in the $\epsilon'(T)$ curve at $T_{max} \sim 190$ K increases and shifts to lower temperature with decreasing frequency, while the peak in the $\epsilon''(T)$ curve decreases more significantly, shifts to lower temperature and below a characteristic freezing temperature $T_f \sim 182$ K becomes essentially frequency independent [Fig. 3(b)]. The frequency independence may reflect a freezing into a glassy state and the onset of nonergodicity in the system.[24] Similar dielectric behavior has been observed in PMN and other perovskite relaxor ferroelectrics.[1–6,25] At 1 MHz and lower, the relaxation process dominating around 150 K also manifests itself in the dielectric losses near T_{max}. The $\epsilon''(T)$ curve for 1 MHz strongly broadens and the inflection points of $\epsilon''(T)$ at the high-temperature side correspond to T_C and 175 K. Most probably, in the vicinity of 175 K a peak in $\epsilon''(T)$ due to the relaxation process dominating around 188 K is still noticeable.

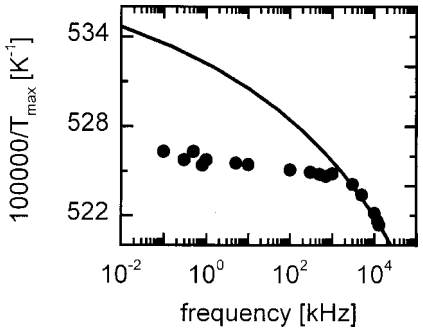

FIG. 4. Inverse temperature of the permittivity maximum ($1/T_{max}$) as a function of the measurement frequency for $Cd_2Nb_2O_7$ around 188 K. The dots are the experimental data. The solid line is the best fit to the Vogel–Fulcher relationship.

To characterize the relaxor state around 188 K, the frequency dispersion of $1/T_{max}$ and ϵ'' was analyzed from the viewpoint of developing the nonexponential dielectric response (non-Arrhenius behavior) and broadening the relaxation-time distribution (non-Debye behavior) near T_f. The nonexponential slowing down of the relaxation rate with decreasing temperature (Fig. 4) was modeled with the Vogel–Fulcher (VF) relationship:

$$f = f_0 \exp[-E_a/k(T - T_f)], \tag{1}$$

where E_a is an activation energy, T_f a freezing temperature, f_0 the Debye frequency related to the nature of relaxation, and k the Boltzmann constant. The best fit to Eq. (1) was obtained for E_a, f_0, and T_f equal to 0.01 eV, 1.9×10^{12} Hz, and 183 K, respectively. Both the activation energy and preexponential factor are proper for a thermally activated process. The value of T_f agrees with the temperature at which ϵ'' becomes nearly frequency independent [Fig. 3(b)]. The deviation from the VF behavior in the frequency range of 100 Hz–1 MHz can be attributed to an admixture of the relaxation process dominating around 150 K, as discussed above. Fitting the data over the whole frequency range of 100 Hz–13 MHz to Eq. (1) yielded an activation energy of 0.003 eV, a preexponential factor of $\sim 10^{13}$ Hz, and a freezing temperature of 189 K, which are physically unreasonable for the relaxation process dominating around 188 K.

The width of the absorption curves, $\epsilon''(f)$, at the low-frequency side increases and tends to flatten out on cooling through T_f, while the shift of f_{max} down in frequency dramatically slows down (Fig. 5). This implies that dramatic broadening occurs in the relaxation-time distribution near T_f, which cannot be attributed to a normal Debye-like (single-relaxation rate) behavior. The relaxation-time distribution, $G(\tau, T)$, can be calculated using Eq. (2)[24,25] based on the assumption that nonexponential dielectric/magnetic response of the dipolar/spin glasses is due to a heterogeneous distribution of independently relaxing regions[26,27]

$$\epsilon''(T, \tau) = \epsilon_0'(T) G(\tau, T), \tag{2}$$

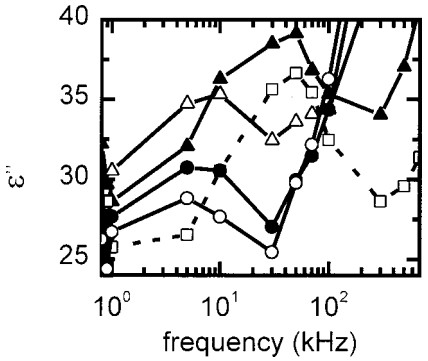

FIG. 5. Dielectric absorption spectra for $Cd_2Nb_2O_7$ at various temperatures around $T_f = 183$ K. The temperatures are 193.2 (dashed line), 190.3, 182, 175.3, and 171.9 K (solid lines), from top to bottom.

where $\epsilon_0'(T)$ is the low-frequency limit of $\epsilon'(T,f)$, and $\tau = f^{-1}$. Assuming $\epsilon_0'(T)$ to be $\epsilon'(T)$ at 100 Hz, the distribution functions, $G(\tau_0,T)$, over the temperature range of 90–300 K were estimated at various measurement frequencies (Fig. 6). The relaxation-time distribution distinctly exhibits that two dielectric relaxation processes develop in the ferroelectric phase of $Cd_2Nb_2O_7$. One of them is characterized by a sharp and rather intensive peak in $G(\tau_0,T)$ which appears just below T_C [Fig. 6(a)]. The peak rapidly shifts to lower temperatures and narrows with decreasing frequency, with its shape changing insignificantly, which is typical of a Debye-like relaxational process. Another process manifests itself as a sharp step in $G(\tau_0,T)$ near T_{max}, with the distribution essentially flat at lower temperatures, over the frequency range investigated [Fig. 6(b)]. Below T_f, the distribution remains very broad and independent on frequency and temperature, which cannot be assigned to a Debye-like relaxation. Above T_f, the magnitude of $G(\tau_0,T)$ increases with increasing frequency, while the edge of the distribution moves to higher temperatures, analogous to a Debye-like relaxation. The deviations from Arrhenius and Debye behavior due to a strong broadening of the relaxation-time distribution near T_f give evidence for a dipolar glass-like behavior of the relaxor ferroelectric $Cd_2Nb_2O_7$ in the state developing below $T_{max} \sim 190$ K.

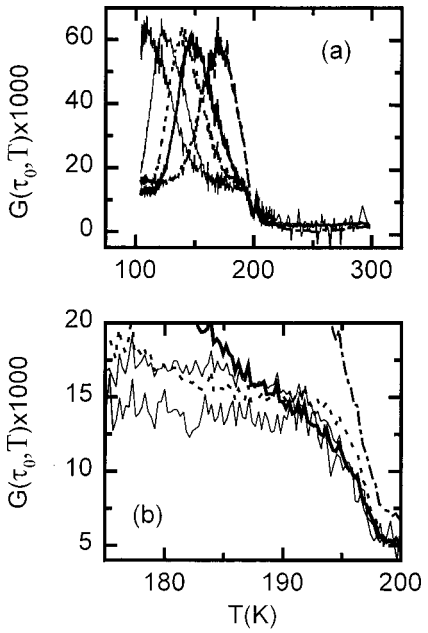

FIG. 6. (a) Relaxation-time distribution $[G(\tau_0,T)]$ for $Cd_2Nb_2O_7$ as a function of temperature at various measurement frequencies. The measurement frequencies are 0.8, 10, 100, 300, and 3000 kHz, from left to right. (b) $G(\tau_0,T)$ as a function of temperature around 188 K at various measurement frequencies: 0.8 (solid, down), 10 (solid, upper), 100 (dot), 300 (solid, thick), and 3000 (dash dot).

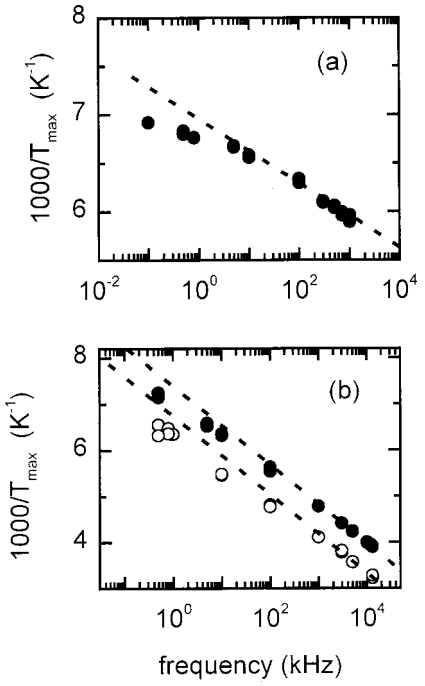

FIG. 7. Inverse temperature of the permittivity maximum ($1/T_{max}$) as a function of the measurement frequency: (a) for $Cd_2Nb_2O_7$ around 150 K, (b) for $Cd_{1-z}Fe_z^{2+}Nb_2O_6$ (upper), and $Cd_{1-y}Fe_y^{3+}Nb_2O_6$ (down) between 100 and 300 K. The dots are the experimental data and the dashed lines indicate Arrhenius-like behavior.

For the dielectric response around 150 K, the peak permittivity significantly changes and shifts to lower temperature with decreasing frequency, but no signs for the value of $\epsilon''(T)$ to become frequency independent are revealed (Fig. 3). The dispersion of inverse temperature of the permittivity maximum shows a moderate deviation from Arrhenius-like behavior [Fig. 7(a)]. The non-Arrhenius response is also announced as an asymmetrical peak in the frequency-dependent dielectric loss [Fig. 8(a)]. On a double-logarithmic plot as shown, the negative inclination of the curves with slope of -1 at high frequencies transforms to a slope of $+\alpha$ at low frequencies, which indicates Curie–von Schweidler relaxation behavior[27] [$\epsilon''(f) \sim (f/\tau)^{-\alpha}$, where τ^{-1} is a relaxation rate, f frequency]. With decreasing temperature, the dielectric absorption curves demonstrate unambiguous increasing of the asymmetry and a tendency to flatten out at the low-frequency side, without freezing the peak-absorption frequency (f_{max}). Similar behavior has been observed in various glass-forming liquids and crystalline materials at temperature far above T_{glass} (a glassy PT temperature point).[4,26–30] The relaxation-time distribution [an intensive peak in the $G(\tau_0,T)$ curves] indicates that for this state a

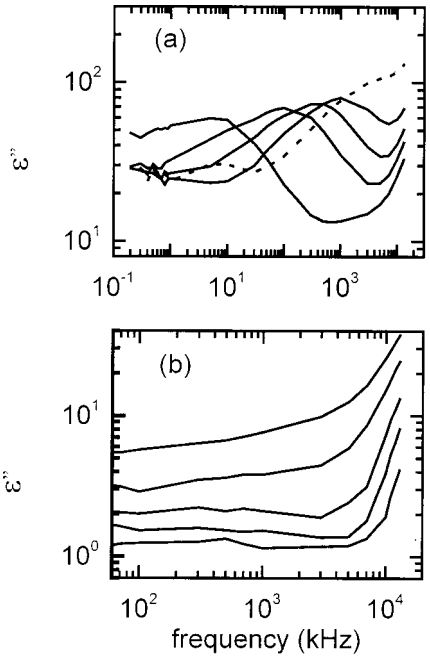

FIG. 8. Log–log plot of dielectric absorption (ϵ'') as a function of frequency for $Cd_2Nb_2O_7$ at various temperatures. The temperatures are (a) 120, 140, 150, 160, and 175 K (around 150 K, $T<T_C$), and (b) 205, 210, 221, 232, and 280 K ($T>T_C$), from left to right.

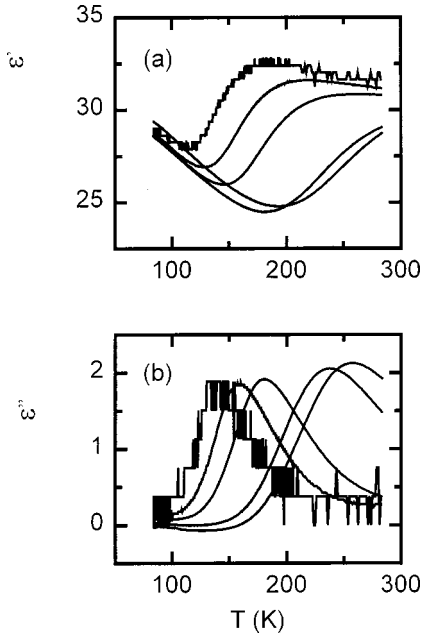

FIG. 9. Weak-field real (a) and imaginary (b) parts of permittivity as a function of temperature on heating of $Cd_{1-z}Fe_z^{2+}Nb_2O_6$ measured at 0.8, 10, 100, 5000, and 13 000 kHz, from left to right.

relatively strong condensation of the polarization fluctuations may be characteristic [Fig. 6(a)]. The state seems to nucleate in the paraelectric phase, cause the dielectric absorption at frequencies higher than 8 MHz [Fig. 8(b), see also Sec. III D], and gradually evolve to a dipolar glass-like state below $T_{glass}\sim 18$ K.[8]

C. Low-frequency dielectric permittivity of $CdNb_2O_6$ columbite

Figures 9 and 10 show the low-frequency (100 Hz–13 MHz) dielectric response of Fe^{2+}/Fe^{3+} doped $CdNb_2O_6$ columbite as a function of frequency and temperature in the zero-field-cooled regime. The compounds exhibit the dielectric relaxation process substantially developing over the temperature range of 90–300 K in the centrosymmetric (paraelectric) phase. With decreasing frequency, the anomaly in the $\epsilon'(T)$ and $\epsilon''(T)$ curves steadily shifts to lower temperature, whereas the value of ϵ' increases and ϵ'' decreases. No frequency independence of $\epsilon''(T)$ is observed down to 90 K [Figs. 9(b) and 10(b)]. The $\epsilon'(T)$ and $\epsilon''(T)$ curves for $Cd_{1-z}Fe_z^{2+}Nb_2O_6$ columbite are shifted towards lower temperature compared to those for $Cd_{1-y}Fe_y^{3+}Nb_2O_6$, with the value of ϵ' noticeably increasing below ~150 K for both compounds. This enables to suppose an existence of PT at lower temperature (<90 K) in the compounds, which will be discussed elsewhere.

The dispersion of $1/T_{max}$ shows a moderate deviation from Arrhenius-like behavior at lower frequencies [Fig. 7(b)]. A non-Arrhenius response is also declared as an asymmetrical peak in the frequency-dependent dielectric loss (Figs. 11 and 12). The dielectric absorption curves demonstrate unambiguous increasing of the asymmetry and a tendency to flatten out at the low-frequency side upon cooling. Yet, freezing the peak-absorption frequency (f_{max}) does not occur, similar to that for $Cd_2Nb_2O_7$ around 150 K. For both compounds, the lower the temperature, the lower the frequency f_{max}, analogous to a Debye-like relaxation behavior. The characteristic frequency of the relaxation for $Cd_{1-z}Fe_z^{2+}Nb_2O_6$ is higher than that for $Cd_{1-y}Fe_y^{3+}Nb_2O_6$ at any temperature (e.g., at 190 K, $f_{max}\sim 30$ kHz for $Cd_{1-y}Fe_y^{3+}Nb_2O_6$ and ~300 kHz for $Cd_{1-z}Fe_z^{2+}Nb_2O_6$).

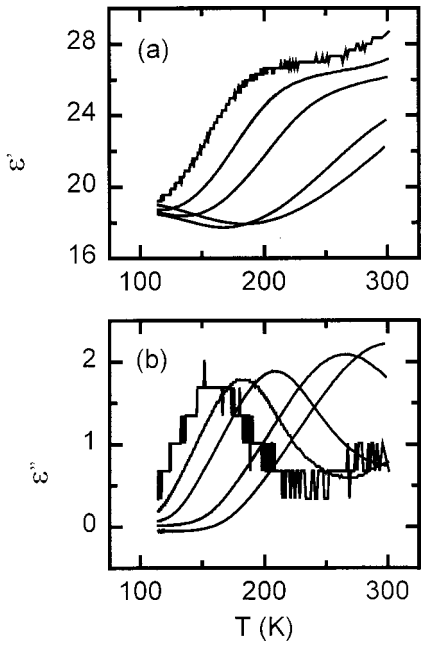

FIG. 10. Weak-field real (a) and imaginary (b) parts of permittivity as a function of temperature on cooling of $Cd_{1-y}Fe_y^{3+}Nb_2O_6$ measured at 0.8, 10, 100, 3000, and 13 000 kHz, from left to right.

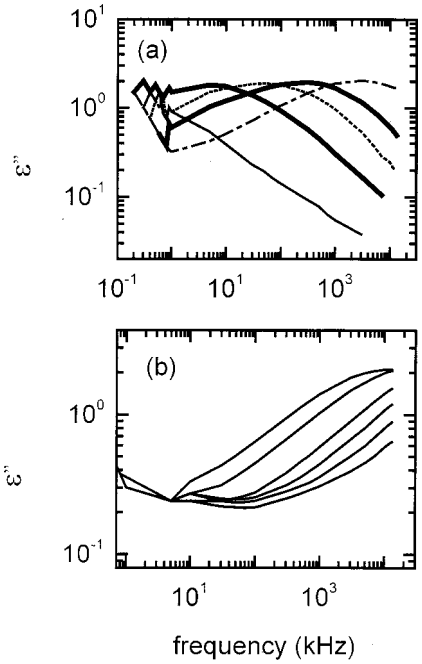

FIG. 11. Log–log plot of dielectric absorption (ϵ'') as a function of frequency for $Cd_{1-z}Fe_z^{2+}Nb_2O_6$ at 120, 150, 172, 190, and 225 K for top, and at 250, 270, 304, 326, 350, and 376 K for bottom, from left to right.

The relaxation-time distribution is characterized by a sharp peak in the $G(\tau_0,T)$ curves (Fig. 13). With decreasing frequency, the peak pronouncedly shifts to lower temperatures and narrows, but its shape changes slowly, which indicates that there is a strong condensation of the polarization fluctuations. The dielectric behavior observed is typical of glass-forming systems at temperature far above T_{glass},[4,26–30] so a predisposition of the Fe^{2+}/Fe^{3+} doped $CdNb_2O_6$ columbite to a formation of a dipolar glassy state at lower temperatures ($T<90$ K) is not excluded.

To obtain more information about the nature of the dielectric relaxation in $Cd_2Nb_2O_7$ in the centrosymmetric phase and to understand the role of the local disorder on the Cd sites in the relaxor and glassy behavior of $Cd_2Nb_2O_7$ and Fe^{2+}/Fe^{3+} doped $CdNb_2O_6$, the complementary dielectric dispersion measurements at higher frequencies and higher temperatures were performed.

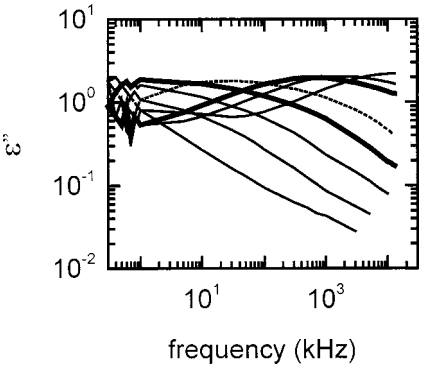

FIG. 12. Log–log plot of dielectric absorption (ϵ'') as a function of frequency for $Cd_{1-y}Fe_y^{3+}Nb_2O_6$ at 120, 135, 150, 170, 190, 250, and 298 K, from left to right.

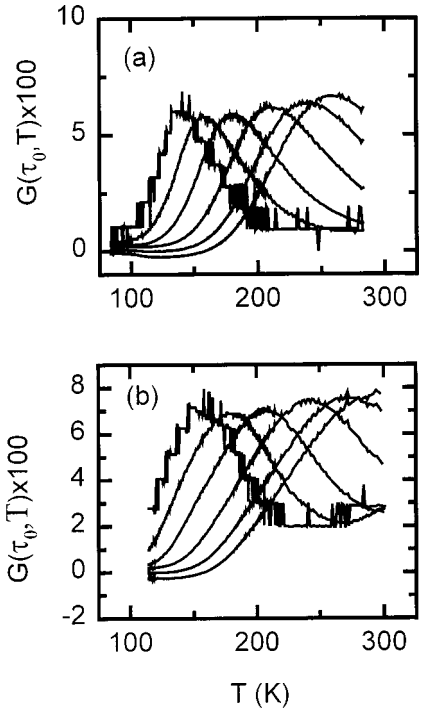

FIG. 13. (a) Relaxation-time distribution $[G(\tau_0,T)]$ for $Cd_{1-z}Fe_z^{2+}Nb_2O_6$ (a) and $Cd_{1-y}Fe_y^{3+}Nb_2O_6$ (b) as a function of temperature at various measurement frequencies. The measurement frequencies are 1, 10, 100, 1000, 5000, and 13 000 kHz, from left to right.

D. High-frequency dielectric permittivity

The HF (1 MHz–1.8 GHz) dielectric spectra of the compounds for two temperatures close to T_{tr} (see Fig. 2) are presented in Figs. 14 and 15. At 341 K, the characteristic frequency of the relaxation is of ~60 MHz for $Cd_{1-y}Fe_y^{3+}Nb_2O_6$ and ~250 MHz for $Cd_{1-z}Fe_z^{2+}Nb_2O_6$,

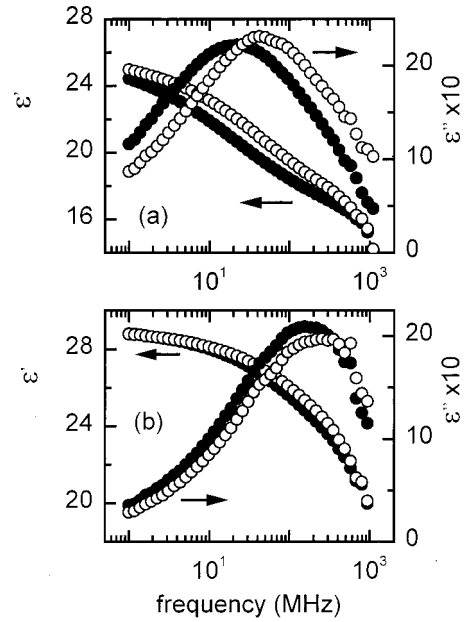

FIG. 14. Dielectric spectra of $Cd_{1-y}Fe_y^{3+}Nb_2O_6$ (a) and $Cd_{1-z}Fe_z^{2+}Nb_2O_6$ (b) over the frequency range of 1 MHz–1.8 GHz at 310 and 341 K for (a), and at 316.5 and 341 K for (b), from left to right.

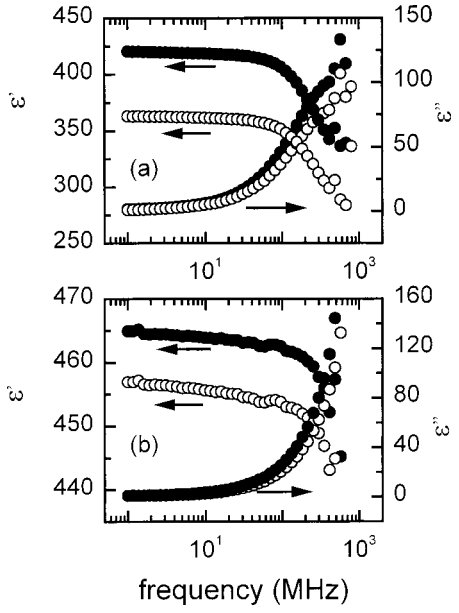

FIG. 15. Dielectric spectra of $Cd_2Nb_2O_7$ (a) and $Cd_2Ta_2O_7$ (b) over the frequency range of 1 MHz–1.8 GHz at 311 and 336 K, from top to bottom for $\epsilon'(f)$, from left to right for $\epsilon''(f)$.

while for $Cd_2Nb_2O_7$ and $Cd_2Ta_2O_7$ the frequency is higher than 500 MHz and 1 GHz, respectively. The peak in the $\epsilon''(f)$ curves and the step in the $\epsilon'(f)$ curves move towards higher frequencies with increasing temperature, with the frequency width of the dispersion curves gradually decreasing. Nevertheless, the width remains much broader than the 1.14 decades expected for a monodispersive Debye-type relaxation of noninteracting dipoles. No remarkable changes in the polydispersive dielectric response of the systems were observed upon coming through T_{tr}. This suggests that no symmetry breaking occurs at T_{tr}, which agrees, at least for $Cd_2Nb_2O_7$ and $Cd_2Ta_2O_7$, with the x-ray data.[21,23] The occurrence of the dielectric relaxation in the centrosymmetric phase of the compounds can be ascribed to a formation of the dynamically reoriented dipoles due to dynamical off-center location of Cd ions[21] and a change in the polarizability of the dipoles in an external ac electric field.

E. Discussion

The comparison of $Cd_2Nb_2O_7$ pyrochlore with $CdNb_2O_6$ columbite seems to be advantageous in that both compounds are composed of the same ions, whereas a columbite structure is more favorable to the highly distorted pyrochlore structure (e.g., in the case of $Cd_2Nb_2O_7$ modified by partial substitution of other ions for Cd^{2+}). The pyrochlore structure ($Fd3m$-O_h^7) and columbite structure ($Pnca$-D_{2h}^{14}) are described by the centrosymmetric space groups.[19] Both structures are formed by $(NbO_6)^{n-}$ octahedra, but the site symmetry for Nb^{5+} is lowered from D_{3d} in the pyrochlore to C_1 in the columbite.[19] The site symmetry for Cd^{2+} is lowered from D_{3d} in the pyrochlore to C_2 in the columbite. In addition, in $Cd_2Nb_2O_7$ these ions are located within $(CdO_8)^{n-}$ scalenohedra, while in $CdNb_2O_6$ they are located within $(CdO_6)^{n-}$ octahedra. The pyrochlore structure can be described as two interpenetrating networks formed by $(NbO_6)^{n-}$ and $(CdO_8)^{n-}$ polyhedra respectively,[7,10,15] with the former being ferroelectrically active.[16,20] The columbite structure is described as a hexagonal closely packed network of oxygen ions with the $(CdO_6)^{n-}$ octahedra-formed layer and two $(NbO_6)^{n-}$ octahedra-formed layers alternating along the z axis.[19]

In the centrosymmetric phase both of $Cd_2Nb_2O_7$ and $Cd_2Ta_2O_7$, the dynamical off-center Cd^{2+} displacements (at 0.1 Å at RT)[21] are supposed to originate the randomly oriented mobile O(7th)–Cd–O(7th) dipoles and, as a consequence, the randomly oriented polarization. In an external ac electric field, the orientational polarizability of the dipoles is heterogeneous and depends on temperature and the ac electric field strength and frequency. For $Cd_2Nb_2O_7$, below T_C a disorder in the orientational polarization of the dynamically reoriented dipoles is supplemented by that of the dipoles originated from the randomly frozen Cd ions in the off-center position. Both types of the off-center location of Cd ions cause a disorder in the $(CdO_8)^{n-}$ network, act as a random field and seem to be responsible for the relaxor and glassy behavior of the system upon cooling (around 188 and 150 K).

Unlike columbite minerals $(Fe,Mn)(Nb,Ta)_2O_6$ and $FeNb_2O_6$, in $CdNb_2O_6$ columbite the ionic sizes of Cd^{2+} and Nb^{5+} differ essentially. The difference causes initial deformation strains in the $(CdO_6)^{n-}$ octahedra, which, in turn, induces the slightly polarized Cd–O dipoles. For Fe^{2+}/Fe^{3+} doped $CdNb_2O_6$ columbite, because of a larger size of Cd^{2+} ions compared to Fe^{2+} or Fe^{3+}, the local deformation strains arise in the $(CdO_6)^{n-}$ octahedra occupied by Fe ions, which forces a random off-center displacement of the latter. The displacements induce the distortion in the O^{2-} environment of the Fe ions and give rise to formation of the randomly oriented Cd–O dipoles and the randomly oriented deformational polarization in the system. The deformational polarizability of the Cd–O dipoles changes under the ac electric field strength and frequency and with decreasing temperature. The local heterogeneity and disorder in the $(CdO_6)^{n-}$ network caused by the off-center displacements of Fe ions seem to act as a random field upon cooling and are responsible for the dielectric relaxation behavior in the centrosymmetric phase typical of the dipolar glass-forming systems far above T_{glass}. Besides, a contribution of the space-charge polarization induced by the difference in the valency of Cd^{2+} and Fe^{3+} (or/and of Fe^{2+} and Fe^{3+}) ions is also not excluded. However, understanding of the role of this mechanism in the dielectric relaxation behavior of Fe^{2+}/Fe^{3+} doped $CdNb_2O_6$ columbite needs further study.

IV. CONCLUSION

The attempt to obtain a highly distorted $Cd_2Nb_2O_7$ pyrochlore modified with the A-site Fe^{2+} or Fe^{3+} ions at $x(Fe)=0.5$ was made, which enabled us (i) to ascertain that $Cd_2Nb_2O_7$ pyrochlore could not tolerate the substitution of 25 mol % Fe^{2+} or Fe^{3+} for Cd^{2+}, (ii) to gain the $CdNb_2O_6$ columbite doped with Fe^{2+} or Fe^{3+} ions on the Cd^{2+} sites

(<8 mol %), and (iii) to compare the dielectric relaxation behavior of $Cd_2Nb_2O_7$ pyrochlore and Fe^{2+}/Fe^{3+}-doped $CdNb_2O_6$ columbite.

The evidence for a dipolar glass-like behavior of the relaxor ferroelectric $Cd_2Nb_2O_7$ in the vicinity of $T_{max} \sim 190$ K is presented. Near the characteristic freezing temperature of the zero-field-cooled state ($T_f = 183$ K) the dielectric absorption spectra and the relaxation-time distribution strongly broaden and tend to flatten out. Below T_f, the peak-absorption frequency (f_{max}) freezes and the imaginary part of the dielectric permittivity becomes frequency independent. Additionally, just below $T_C = 196$ K $Cd_2Nb_2O_7$ exhibits the dielectric relaxation caused by the ferroelectric domain wall motions in a weak ac electric field. The dielectric response of $Cd_2Nb_2O_7$ dominating far below T_C (around 150 K) and that of Fe^{2+}/Fe^{3+}-doped $CdNb_2O_6$ between 90 and 380 K are typical of glass-forming systems at temperature far above T_{glass}. It is proposed that although the nature of structural disorder in $Cd_2Nb_2O_7$ pyrochlore and Fe^{2+}/Fe^{3+}-doped $CdNb_2O_6$ columbite is different, in both systems the off-center displacements of the A-site ions act as a random field and are responsible for the relaxor and dipolar glass-like behavior upon cooling. The comparison of the HF (1 MHz–1.8 GHz) dielectric relaxation in $Cd_2Nb_2O_7$ and its isostructural analog $Cd_2Ta_2O_7$ at RT and higher was made. The Debye-like dielectric relaxation in the centrosymmetric phase of both pyrochlores can be attributed to a formation of the dynamically reoriented O(7th)–Cd–O(7th) dipoles due to dynamical off-center displacements of Cd ions, with the orientational polarizability of the dipoles changing in the external ac electric field.

ACKNOWLEDGMENTS

This work was sponsored by the RFFI under Grant No. 0002-16900 and the J. Mianowski Fund.

[1] L. E. Cross, Ferroelectrics **76**, 241 (1987); **151**, 305 (1994).
[2] D. Viehland, M. Wuttig, and L. E. Cross, Ferroelectrics **120**, 71 (1991); D. Viehland and J.-F. Li, J. Appl. Phys. **75**, 1705 (1994).
[3] J. Toulouse and R. Pattnaik, J. Korean Phys. Soc. **32**, S942 (1998).
[4] W. Kleemann, J. Korean Phys. Soc. **32**, S939 (1998).
[5] A. Levstik, Z. Kutnjak, C. Filipic, and R. Pirc, J. Korean Phys. Soc. **32**, S957 (1998).
[6] R. Farhi, M. Marssi, R. Cleveland, M. Kosec, and B. Malic, Ferroelectrics **236**, 169 (2000).
[7] N. N. Kolpakova, M. Wiesner, G. Kugel, and P. Bourson, Ferroelectrics **201**, 107 (1997); **190**, 179 (1997).
[8] N. N. Kolpakova, I. L. Shul'pina, M. P. Shcheglov, S. Waplak, W. Bednarski, W. Nawrocik, and M. Wiesner, Ferroelectrics **240**, 265 (2000).
[9] Ch. Ang, L. E. Cross, R. Guo, and A. S. Bhalla, Appl. Phys. Lett. **77**, 732 (2000); Ch. Ang, R. Guo, A. S. Bhalla, and L. E. Cross, J. Appl. Phys. **87**, 7452 (2000).
[10] N. N. Kolpakova, R. Margraf, and M. Polomska, J. Phys.: Condens. Matter **6**, 2787 (1994).
[11] N. N. Kolpakova, M. Wiesner, A. O. Lebedev, P. P. Syrnikov, and V. A. Khramtsov, Tech. Phys. Lett. **24**, 679 (1998).
[12] I. L. Shul'pina, N. N. Kolpakova, M. P. Shcheglov, and A. O. Lebedev, Tech. Phys. Lett. **25**, 561 (1999).
[13] S. L. Swartz, C. A. Randall, and A. S. Bhalla, J. Am. Ceram. Soc. **72**, 637 (1989).
[14] R. D. Shannon, Acta Crystallogr. A **32**, 751 (1976).
[15] R. A. McCauley, J. Appl. Phys. **51**, 290 (1980).
[16] E. Aleshin and R. Roy, J. Am. Ceram. Soc. **45**, 18 (1962).
[17] F. Brisse, D. J. Stewart, V. Seidl, and O. Knop, Can. J. Chem. **50**, 3648 (1972).
[18] *The Minerals*, edited by the Academy of Sciences of the USSR (Nauka, Moscow, 1967), Vol. 2, pp. 148 and 303.
[19] *Structurbericht*, edited by C. Hermann, O. Lohrmann, and H. Philipp (Akademische, Leipzig, 1937), Vol. 2, pp. 55 and 337.
[20] A. W. Sleight and J. D. Bierlein, Solid State Commun. **18**, 163 (1976).
[21] K. Lukaszewicz, A. Pietraszko, J. Stepien-Damm, and N. N. Kolpakova, Mater. Res. Bull. **29**, 987 (1994).
[22] V. A. Isupov and O. K. Khomutetskii, J. Tech. Phys. **27**, 2513 (1957).
[23] N. N. Kolpakova, A. Pietraszko, S. Waplak, and L. Szczepanska, Solid State Commun. **79**, 707 (1991).
[24] E. Courtens, Phys. Rev. Lett. **52**, 69 (1984).
[25] D. Viehland, S. Jang, L. E. Cross, and M. Wuttig, Philos. Mag. B **64**, 335 (1991).
[26] R. Chamberlin, J. Appl. Phys. **76**, 6401 (1994).
[27] R. Chamberlin, Phase Transitions **65**, 169 (1998).
[28] P. Lehnen, J. Dec, W. Kleemann, Th. Woike, and R. Pankrath, Ferroelectrics **240**, 281 (2000).
[29] B.-G. Kim, J.-J. Kim, D.-H. Kim, and H. M. Jang, Ferroelectrics **240**, 249 (2000).
[30] S. Benkhof, T. Blochowicz, A. Kudlik, C. Tschirwitz, and E. Rössler, Ferroelectrics **236**, 193 (2000).